Analysis of Slot Injection in Hypersonic Flow

J. A. Schetz,* F. S. Billig,† and S. Favin‡
Johns Hopkins University, Applied Physics Laboratory, Laurel, Maryland 20707

The aim of this work was to develop a relatively simple, but reliably accurate, analysis for the major features of the flowfield produced by supersonic, tangential slot injection into a hypersonic (or supersonic) external flow including the effects of turbulent mixing, viscid/inviscid interaction, initial pressure mismatch, thick boundary layers, skin friction and wall heat transfer, and heat release for reactive injectants. The analysis developed uses hypersonic (or supersonic) small perturbation theory; entrainment models including the effect of a convective Mach number; a quasi-one-dimensional assumption in the mixing and burning region; an instantaneous, one-step heat release model; and simple representations of skin friction and heat transfer. Good agreement with available experiments for gross flowfield variables such as $p(x)$, $A(x)$, $T_0(x)$, $M(x)$, etc., is demonstrated. The calculation used about 2 s of CPU time on an Amdahl 5890 class computer. Finally, some predictions for combustor flowfield development for a generic hydrogen-fueled scramjet vehicle at flight Mach numbers of 10, 15, and 20 are presented and discussed. A realistic range of values for boundary-layer thickness, slot height, injection Mach number, and total temperature is considered.

Nomenclature

A	= area of the one-dimensional viscous region
a	= slot height
C_{1-4}	= mixing rate constants
C_f	= skin friction coefficient based on one-dimensional variables
C_p	= specific heat
$\dot{m}/dx$	= entrainment rate
F_{RA}	= Reynolds analogy factor
f_s	= stoichiometric fuel/air ratio
h_f	= heating value of the fuel
H	= stagnation enthalpy
$\dot{m}$	= one-dimensional average mass flow
M_j	= slot injection Mach number
M_1	= freestream Mach number
$M(x)$	= one-dimensional average Mach number
p	= static pressure
Pr	= Prandtl number
q_w	= wall heat transfer rate
St	= Stanton number
T	= one-dimensional average static temperature
T_{aw}	= adiabatic wall temperature
$T_0(x)$	= one-dimensional average total temperature
T_w	= wall temperature
U	= one-dimensional average velocity
x	= streamwise coordinate
x_{pc}	= potential core length
W	= molecular weight
γ	= ratio of specific heats
θ	= local flow angle
ϕ	= equivalence ratio
δ_i	= initial boundary-layer thickness

Subscripts

1	= external flow quantities
2	= quantities in the one-dimensional viscous region
j	= jet exit conditions

Received June 7, 1989; revision received October 27, 1989.

*Consultant; also W. Martin Johnson Professor and Department Head, Aerospace and Ocean Engineering Department, Virginia Polytechnic Institute and State University. Fellow AIAA.
†Chief Scientist, Aeronautics Department. Fellow AIAA.
‡Senior Programmer.

Introduction

THE flowfield produced by sonic or supersonic wall slot injection parallel to a supersonic or hypersonic mainstream is complex from the viewpoint of detailed analysis due to the likelihood of wave patterns superimposed upon a viscous mixing zone. If the flow is turbulent, there are important turbulence modeling issues, mainly in the areas of modeling merging mixing zones and the development of a nominally free shear layer beneath a possibly large freestream side initial boundary layer.

There are attractive practical applications of this flow arrangement (e.g., separation prevention, thermal protection, and skin friction reduction), and so a number of experiments (e.g., Refs. 1-10) and analyses (e.g., Refs. 3, 4, and 11-14) have been presented. One application, fuel injection in scramjet engines, also involves different fluids and chemical reactions, making analysis even more challenging. Nonetheless, several analyses have been developed and published. Some treatments have made numerous and strong simplifying assumptions, such as constant static pressure, which precludes wave patterns and viscid/inviscid interactions. Others retain more of the basic physics of the flow, but these tend to become rapidly complex and costly in terms of computer time and data preparations and interpretation.

One aspect of these flowfields that has received little previous attention is the effects of a large initial boundary layer on the mainstream side. Many practical cases involve situations where the ratio of the initial boundary-layer thickness to the slot height can be very large, i.e., $\delta_i/a \gg 1$. In scramjets, for example, this ratio can have a value of 10. Indeed, a number of the slot injection experiments in the literature have large values of this ratio (Ref. 9 and $\delta_i/a \approx 4$). Under such circumstances, one can expect that the initial boundary layer plays a dominant role in the slot injection flowfield development, especially in the near field. Any explicit effects of the initial boundary layer have only been infrequently (e.g., Refs. 4 and 11) treated.

An area where the important influence of an initial boundary layer has arisen is in turbulence modeling for high Mach number flows. A number of workers[15-18] have identified a "convective" Mach number effect on mixing rates in shear layers when the initial boundary layer is small. More recent studies have shown that this effect is only operative beyond $x \approx 25\delta_i$. If δ_i is large compared to a, then $25\delta_i$ may be as large as $250a$ so that the convective Mach number influence can be unimportant from a practical standpoint.

Despite all of the complications that have just been introduced, there remains a need for simple, inexpensive, reasonably accurate calculation methods that can be used for design purposes where numerous calculations are required. For design purposes, the output needed are not detailed profiles, but rather reliable predictions of gross flowfield quantities such as the total amount of mainstream fluid entrained into the mixing zone for mixing studies or thermal protection or the length of the flame in the scramjet combustor application mentioned above. These considerations suggest a helpful role for a "simplified" analysis that retains at least approximate models of all of the basic physics and chemistry of the flow. Earlier, we had developed such treatments for the different, but related, flow problem of base injection and burning behind high-speed vehicles.[19-21] These proved quite successful at predicting the main features of those flows at a very low cost. The principal simplifying features of those analyses were the adoption of a one-dimensional representation for the flow in the viscous region and the use of linearized supersonic theory to describe the inviscid/viscous interaction. More recently, the same general ideas were extended to slot injection flows without including any explicit effects of an initial boundary layer.[22] Generally good agreement was found between predictions and experiments, although we found that the agreement was poorer in cases where the initial boundary layer in the experiment was large (e.g., Refs. 9 and 10). Thus, it was decided to develop a new analysis that would directly include the influences of this important variable.

Analysis

The development of the analysis involves numerous choices of approximations and models. Although some rationale for each choice is given, the adequacy of the final procedure can best be judged only by comparisons of predictions with experiments for a number of different cases.

Formulation

Some simplifications must be introduced to achieve the stated goal of an inexpensive calculation procedure. Following the ideas behind our earlier work, a viscous mixing zone is represented as a one-dimensional flow region with suitably averaged (across the flow) quantities varying only in the streamwise direction. There is turbulent entrainment of surrounding fluid into this region, and the static pressure is determined by an inviscid/viscous interaction with the surrounding flow. Also, here skin friction and wall heat transfer are important, which was not the case for the base flow problem. A "modular" approach was adopted, where the flows in different subregions of the general flowfield are treated separately, and then the solutions are joined together to produce a composite whole.

Consider the flowfield as sketched in Fig. 1, where it is presumed that the thickness of the boundary layers on the internal surfaces of the slot nozzle are small compared to either the slot height or the mainstream side boundary layer. That is true in many practical situations. There is then a "potential" or inviscid core in the slot exit flow that occupies most of the slot height. Beyond the slot lip end ($x \geq 0$), there is entrainment into the main mixing region both from the external stream and the slot exit flow. There is also entrainment from the potential core of the slot exit flow into the growing boundary layer on the bottom wall. When all of the flow in the slot exit potential core has been entrained into either the main mixing zone or the wall boundary layer, the potential core disappears at $x = x_{pc}$.

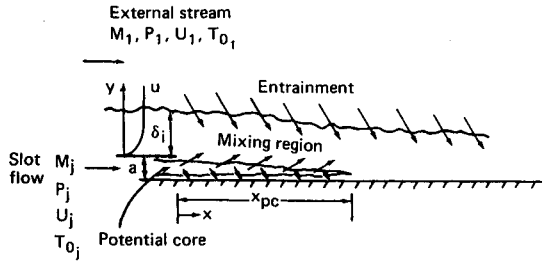

Fig. 1 Schematic of the slot injection flowfield.

Consider the flow in the main mixing region as one-dimensional with suitably averaged variables. With that and taking γ and γ_2 as constants, the energy and streamwise momentum equations can be combined to give

$$\frac{dM^2}{dx} = \frac{-2M^2\left(1+\frac{\gamma_2-1}{2}M^2\right)}{(1-M^2)}\left\{\frac{1}{A}\frac{dA}{dx} - \frac{1+\gamma_2 M^2}{2}\frac{1}{T_0}\frac{dT_0}{dx}\right.$$

$$+\left[\gamma_2 M u_1\left(\frac{1+\frac{\gamma_2-1}{2}M^2}{\gamma_2/W\,T_0}\right)^{1/2} - (1+\gamma_2 M^2)\right]\frac{1}{\dot{m}}\frac{d\dot{m}}{dx}$$

$$\left.-\frac{C_f\gamma_2 M^2}{2A} + \frac{(1+\gamma_2 M^2)}{2\left(1+\frac{\gamma_2-1}{2}M^2\right)}\frac{1}{W}\frac{dW}{dx}\right\} \tag{1}$$

Note that the only shear involved is the wall shear which does not act on the flow in the main mixing region for $x < x_{pc}$, so the next to the last term in Eq. (1) is zero for $x < x_{pc}$. The area A is the transverse height (in the two-dimensional planar case) of the main viscous region. Turbulence is manifested only as an entrainment rate $d\dot{m}/dx$ which has two parts, $(d\dot{m}/dx)_{\text{inner}}$ and $(d\dot{m}/dx)_{\text{outer}}$ for $x < x_pc$.

The continuity equation and the equation of state give, with a perfect gas, the pressure variation in the viscous region as

$$\frac{1}{p}\frac{dp}{dx} = \frac{1}{\dot{m}}\frac{d\dot{m}}{dx} - \frac{1}{A}\frac{dA}{dx} - \frac{1}{2}\frac{1}{M^2}\left[\frac{1+(\gamma_2-1)M^2}{1+\left(\frac{\gamma_2-1}{2}\right)M^2}\right]\frac{dM^2}{dx}$$

$$+\frac{1}{2}\frac{1}{T_0}\frac{dT_0}{dx} - \frac{1}{2}\frac{1}{W}\frac{dW}{dx} \tag{2}$$

The external flow is taken as inviscid with the static pressure determined by the hypersonic small disturbance theory for compression[23]

$$\frac{dp}{p} = \gamma M_1\left[1+\frac{\gamma+1}{2}M_1\theta + \frac{\gamma+1}{4}(M_1\theta)^2\right]d\theta \tag{3}$$

It is assumed here that Eq. (3) is an adequate approximation for both compressions and expansions. If $M_1 \leq 2.50$, the corresponding linearized supersonic theory results are used. The inviscid/viscous interaction requires that the right-hand side of Eq. (2) equal that of Eq. (3).

For burning cases, an idealized, diffusion-controlled reaction model is assumed. Thus, as soon as fuel is entrained into the viscous region from the slot flow, it reacts instantly with the main airflow in the main mixing region up to $x = x_{pc}$. A simple heating value representation is also introduced. With all of this

$$\frac{1}{T_0}\frac{dT_0}{dx} = \left[\left(\frac{H_j - C_{pj}T - U^2/2}{C_{p_2}T_0}\right) + \frac{\bar{h}_f}{C_{p_2}T_0}\right]\frac{1}{\dot{m}}\left(\frac{d\dot{m}}{dx}\right)_{\text{inner}}$$

$$+\left(\frac{H_1 - C_{p_1}T - U^2/2}{C_{p_2}T_0}\right)\frac{1}{\dot{m}}\left(\frac{d\dot{m}}{dx}\right)_{\text{outer}} \tag{4a}$$

Heat transfer to or from the wall does not influence the flow in the main mixing region for $x < x_{pc}$.

After the end of the potential core ($x \geq x_{pc}$), the mixing region extends all the way down to the wall, and the only entrainment is from the external stream. Equation (1) still holds, but the C_f term must be included. Equations (2) and (3) also still hold. Equation (4a) must be rewritten as

$$\frac{1}{T_0}\frac{dT_0}{dx} = \left[\left(\frac{H_1 - C_{p_1}T - U^2/2}{C_{p2}T_0}\right) + \frac{\bar{h}_f \cdot f_s}{C_{p_2}T_0}\right]\frac{1}{\dot{m}}\frac{d\dot{m}}{dx} + \frac{C_f}{2A}\left(\frac{T_w - T_{aw}}{T_0}\right) \tag{4b}$$

where $\bar{h}_f \cdot f_s \approx 1520 - 0.1\,(T_0)$, °R for H_2/air. The last term models wall heat transfer using Reynolds analogy

$$St = (C_f/2) \tag{5}$$

The adiabatic wall temperature is calculated with a recovery factor taken as $Pr^{1/3}$ using M and T_0 in the mixing zone. Some workers[12] report a Reynolds analogy factor greater than unity for slot injection flows. A value of unity was used here. One reason is that the definitions of C_f and St in this work are based on one-dimensional average quantities in the viscous region, not edge values as used in Ref. 12.

Finally, consider how entrainment from the external stream occurs. It is the result of a difference between the local flow angle at the outer edge of the mixing region and the growth rate of the mixing region dA/dx, i.e.,

$$\frac{d\dot{m}}{dx} = \rho_1 u_1\left(\frac{dA}{dx} - \theta\right) \tag{6}$$

This is the easiest to interpret for $x \geq x_{pc}$. Before that, the pressure interaction with the external stream involves only $(d\dot{m}/dx)_{\text{outer}}$ and the A in Eq. (7) must be the total height from the wall up to the outer edge of the main mixing region.

Mathematical Overview

The formulation described above results in six ordinary differential equations for six unknowns: $M(x)$ [actually $M^2(x)$], $\dot{m}(x)$, $T_0(x)$, $\theta(x)$, $A(x)$, and $p(x)$. The six equations are Eq. (1), an entrainment rule yet to be specified, Eq. (4a) or (4b), Eqs. (2) and (3) combined and solved for $d\theta/dx$, Eq. (6) solved for dA/dx, and Eq. (3).

The parameters in the problem are M_1, T_{01}, p_1, δ_i, M_j, T_{0j}, p_j, a, γ_2, C_{p2}, T_w, f_s, and h_f.

The initial conditions required are $M(0)$, $\dot{m}(0)$, $T_0(0)$, $A(0)$, and $p(0) = p_1$. The initial flow angle $\theta(0)$ can be found from p_1, p_j, and Eq. (3). These initial values are to be understood as one-dimensional averages across the initial boundary layer. To find such average values from specified M_1, T_{01}, p_1, δ_i, and T_w, some assumptions are necessary. The approximate expression

$$\frac{u}{u_1} = \left(\frac{y}{\delta_i}\right)^{1/7} \tag{7}$$

and Crocco relations for $H(u)$ were used.

The calculations are run as described above from $x = 0$ until $x = x_{pc}$. At that point, new one-dimensional average values are calculated including now the fluid in the wall boundary layer that has been developing below the potential core (see Fig. 1). These new average values are treated as "initial" conditions for a new calculation begun at $x = x_{pc}$ and continued as far downstream as desired.

For cases with a small, freestream-side boundary layer ($\delta_i/a \ll 1$), the procedure is less complex. The main viscous region is taken as the whole slot flow and the freestream fluid entrained into it from $x = 0$. There is no separate treatment from $x = 0$ to $x = x_{pc}$. The formulation then resembles that for $x \geq x_{pc}$ for cases with large initial boundary layers.

Real Gas Effects

Most practical cases can be analyzed assuming perfect gas behavior throughout. However, for high M_1, the relations relating static and total temperature, for example, are no longer adequate in the mainstream and its boundary layer. For such cases, a table look-up procedure using equilibrium air values for all thermodynamic quantities was adopted here. Also, rather than T_{01}, it is more appropriate to work with the stagnation enthalpy H_1.

The flow in the viscous region is taken as having a constant γ_2. The mixture molecular weight is calculated assuming instantaneous mixing and, if appropriate, reaction to produce products at the local fuel/air ratio. For example, for H_2 injection and burning in air, water is assumed as the only product. Last, the relation $C_{p2} \approx 7/W$ is assumed. Actually, one finds that even scramjet cases for high flight Mach numbers involve one-dimensional average static temperature levels in the mixing region that makes these approximations quite reasonable. Average static temperature levels up to about 2500 K are certainly acceptable.

Turbulence Modeling

The explicit effects of turbulence appear as an entrainment rate $d\dot{m}/dx$ that must be modeled. Actually, relatively few turbulence models are presented in terms of entrainment rates. It is much more common to model an eddy viscosity (or mixing length) or a width-growth rule. In principle, these can be related to one another, but that exercise is not always straightforward or free of additional assumptions. A good starting point for the current purposes is the Crocco-Lees entrainment model,[24] which was developed for boundary-layer flows:

$$\frac{d\dot{m}}{dx} = C_1\rho_1 u_1 \tag{8}$$

with $C_1 \approx 0.015 - 0.03$ (the higher value is for separating flows).

In our earlier work for base injection flows,[19-21] a different model was proposed

$$\frac{d\dot{m}}{dx} = C_2\rho_1 u_1\left|1 - \frac{\overline{\rho u}}{\rho_1 u_1}\right| \tag{9}$$

with $C_2 \approx 0.01 - 0.02$. This was based on a notion suggested first by Ferri.[25] This or any other "difference" model [Δu or $\Delta(\rho u)$] will have difficulty when that difference tends to zero. In any event, Eq. (9) resulted in good predictions for base injection cases.[19-21]

For cases with large initial boundary layers and $x \leq x_{pc}$, the flow is presumed boundary-layer-like, and the Crocco-Lees model was used with $C_1 = 0.02$ as

$$\left(\frac{d\dot{m}}{dx}\right)_{\text{inner}} = C_1\rho_j u_j \tag{10a}$$

and

$$\left(\frac{d\dot{m}}{dx}\right)_{\text{outer}} = C_1\rho_1 u_1 \tag{10b}$$

Recently, experiments on free mixing flows such as shear layers and jets[15-18] have shown a decrease in mixing rate as a function of a suitably defined Mach number of the large-scale structures M_c. Those results have been presented as a width-growth rule[18]:

$$\frac{d\delta_{\text{viz}}}{dx} = C_3 f(M_c)\frac{\left(1 - u_2/u_1\right)\left(1 + \sqrt{\rho_2/\rho_1}\right)}{\left(1 + \frac{\rho_2 u_2^2}{\rho_1 u_1^2}\right)} \tag{11}$$

with $C_3 \approx 0.17$ and $f(M_c)$ is a function equal to unity up to about $M_c = 0.5$ and then decreasing to a value of about 0.3 by

$M_c \approx 1.0$.[15-18] There remain questions as to whether this decrease in mixing occurs in similar flows but where a solid wall was present in the viscous region and/or a large initial boundary layer exists such as for the slot injection flow of concern here. Nonetheless, it is of interest to extend these new results to an entrainment law for use in parametric calculations and comparisons with data. In Eq. (11) and all that follows from it, the subscript 2 must be for the lower speed stream. To illustrate the process of extending a width-growth law to an entrainment law, consider first a case where $\rho_2 = \rho_1$ and $u_2 = 0$ and then assume a linear velocity profile and that the entrainment into one side of a free shear layer is one-half that into the whole. Equation (11) then leads to

$$\frac{d\dot{m}}{dx} = C_4 \rho_1 u_1 f(M_c) \tag{12a}$$

where $C_4 \approx 0.04$, which compares with Eq. (8) when $f(M_c) \approx 1$. For the general case, a comparable development yields

$$\frac{d\dot{m}}{dx} = C_4 f(M_c) \rho_1 u_1 \left[\frac{\frac{\rho_2 u_2}{\rho_1 u_1} + \frac{\frac{u_2}{u_1}\left(1-\frac{\rho_2}{\rho_1}\right)+\frac{\rho_2}{\rho_1}\left(1-\frac{u_2}{u_1}\right)}{2}}{+\frac{\left(1-\frac{u_2}{u_1}\right)\left(1-\frac{\rho_2}{\rho_1}\right)}{3}} \right] \cdot \left[\frac{\left(1-\frac{u_2}{u_1}\right)\left(1+\frac{\rho_2}{\rho_1}\right)}{1+\frac{\rho_2 u_2^2}{\rho_1 u_1^2}} \right] \tag{12b}$$

If $u_2 > u_1$, the subscripts in the last bracket in Eq. (12b) and the definition of M_c must be reversed. In deriving Eq. (12b), it was assumed that both the velocity and density profiles could be represented by linear variations over the width of the vorticity thickness. That is a reasonable assumption for $\rho_2 \leq \rho_1$ but not for $\rho_2 \gg \rho_1$, but most cases of practical interest involve $\rho_2 \leq \rho_1$.

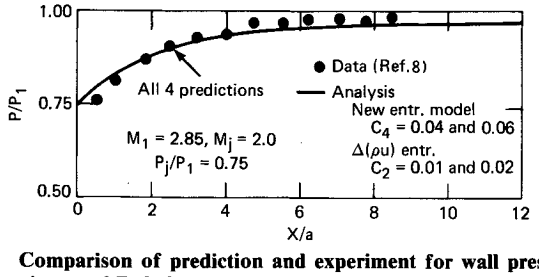

Fig. 2 Comparison of prediction and experiment for wall pressure for experiment of Ref. 8.

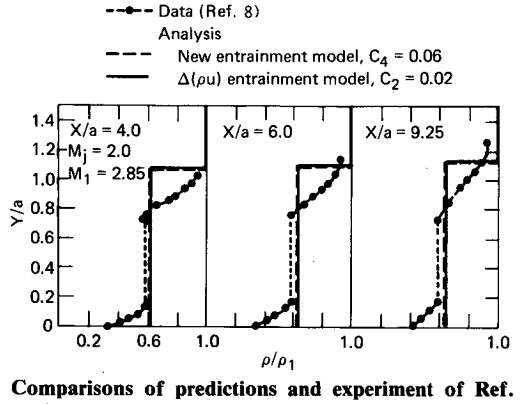

Fig. 3 Comparisons of predictions and experiment of Ref. 8 for density profiles at $x/a = 4.0$, 6.0, and 9.25.

With the assumptions necessary to go from the reported width-growth to the entrainment law needed here, it is good to have some method of checking the result, at least for a limiting case. Brown and Roshko[15] did develop an approximate entrainment law by an entirely different approach. For $u_2 = 0$ and $\rho_2 = \rho_1$, they give

$$\frac{d\dot{m}}{dx} = 0.052\, \rho_1 u_1 \tag{13}$$

which can be compared with our equivalent result from Eq. (12b) of

$$\frac{d\dot{m}}{dx} = 0.06\, \rho_1 u_1 \tag{14}$$

For $(\rho_2/\rho_1) = 1/7$, they deduce a change in the constant in Eq. (13) to 0.038. Equation (12b) gives 0.03. We take this to show rough correspondence, in view of the considerable uncertainties in the constants and the different approximations in both analyses.

By analogy with these results, it is logical to include the same $f(M_c)$ in Eq. (9) as in Eq. (12b) if one believes the effect is significant for wall-bounded flows, i.e.,

$$\frac{d\dot{m}}{dx} = C_2 f(M_c) \rho_1 u_1 \left| 1 - \frac{\overline{\rho u}}{\rho_1 u_1} \right| \tag{15}$$

Comparisons of Predictions with Experiment

To test the adequacy of the analysis, we present several comparisons of predictions and experiment. The first group of cases are for nonreacting fluids. Within that group, the first considered has a very small initial boundary-layer thickness, $\delta_i/a \ll 1$, and involves air injection into air. The next cases have thick boundary layers, and the final nonreacting case involves H_2 injection into air. For reacting cases, two experiments for H_2 injection and burning in air are considered.

Nonreacting Cases

A case from Ref. 8 with $M_1 = 2.85$ and $M(0) = 2$ with air injection into air was considered first and $\delta_i \ll a$. This is an interesting case, since $p_j \neq p_1$. Calculations were made with entrainment modeled with Eq. (9) denoted as "$\Delta(\rho u)$ Entrainment" and Eq. (12b) denoted as "New Entrainment Model" with mixing constant choices of 0.01, 0.02 and 0.04, 0.06, respectively. The predictions and measurements are compared in Fig. 2. One can note the good agreement for both entrainment rate expressions. Density profile comparisons are shown in Fig. 3. The agreement between prediction and experiment is reasonably good. The comparisons do indicate that mixing rate constants on the high side perform better. Based on these results and others, we have selected a value of $C_2 = 0.02$ for Eq. (9) and $C_4 = 0.06$ for Eq. (12b). Also, these experiments had conditions such that $M_c \leq 0.3$ in the whole flowfield, and so the issue of a possible decrease in mixing as a function of M_c was not relevant.

A case from Ref. 10 with $M_1 = 3.0$ and $M_j = 1.7$ ($p_j = 0.8p_1$) and $\delta_i/a = 0.7$ with air injection into air was considered next. A comparison of the predicted and measured Mach number profile at the furthest measured downstream station ($x/a = 20$) is shown in Fig. 4. Note that both the height of the viscous region and the average value of the Mach number are quite accurately predicted. Last, M_c was never greater than 0.2.

Another air/air case but with a larger initial boundary-layer thickness can be found in Ref. 5. The predicted viscous area growth is compared to the data in Fig. 5 where good agreement can be noted. The value of the convective Mach number was low everywhere.

The hot H_2/air slot injection experiment reported in Ref. 9 has a nonburning as well as a burning series with $M_1 = 2.5$,

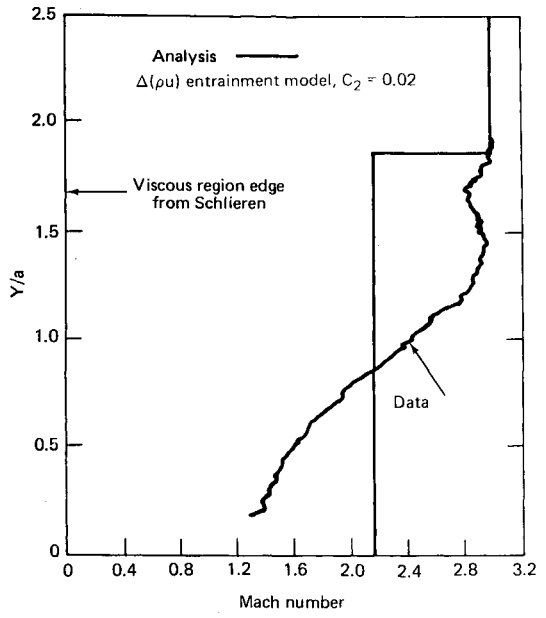

Fig. 4 Comparison of predictions and experiment of Ref. 10 for Mach number profiles at $x/a = 20$, $M_1 = 3.0$, $M_j = 1.7$, $\delta_i/a = 0.6$, and $p_j/p_1 = 0.8$.

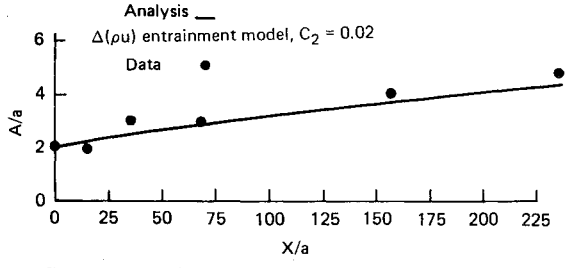

Fig. 5 Comparison of predicted and measured viscous area growth for experiment of Ref. 5; $M_1 = 3.0$, $M_j = 1.0$, $\delta_1/a = 1.05$, and $p_j/p_1 = 1.0$.

$M_j = 1$, and $\delta_i/a = 3.8$. The nonburning data are useful as a next step in complexity in evaluating the current analysis. The nonburning test simply has no O_2 in the vitiated air mainstream. The experiments yielded profiles at $x = 35.6$ cm ($x/a = 89$), and the predictions of the analysis are compared with these results in Figs. 6a–6c. The predictions are seen to be in good agreement with the data for both entrainment models using the higher values of the constants. The height of the mixing region and the one-dimensional average values of M, U, T_0, T, and H_2 concentration are all well predicted. Again, it is important to note that the convective Mach number for this case was never above 0.2.

Burning Cases

An H_2/air burning case is a stringent test against which to judge the adequacy of any viscous flow analysis. The burning experiments of Ref. 9 were used here first. The main differences compared to the case from the same reference discussed in the previous section are a slightly higher air temperature and, more importantly, the presence of oxygen in the external stream. Profile comparisons similar to those for the nonburning case in Fig. 6 are given in Figs. 7a–7c. Again, the predictions are seen to be in rather good agreement with the data. The agreement is better than in Ref. 22 where the effects of the large initial boundary layer were not treated. As before, the convective Mach number is low.

A second H_2/air burning experiment is reported in Ref. 4, although fewer details are available. In particular, the initial boundary-layer thickness was not measured. This case is interesting, however, since it could not be treated in a straightforward manner with the analysis of Ref. 22. Calculations have been made with the current analysis assuming a reasonable range of values of δ_i. Good results were obtained. Some comparisons with experimental observations are shown in Figs. 8 and 9.

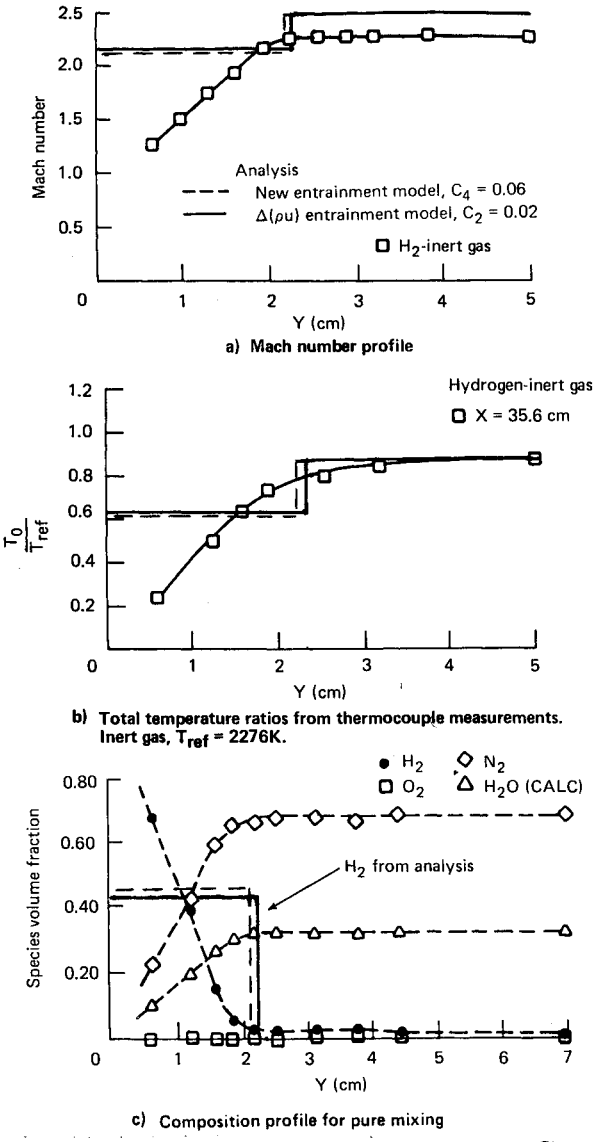

Fig. 6 Comparisons of predictions and data from nonburning H_2/air experiment of Burrows and Kurkov[9]; $M_1 = 2.5$, $M_j = 1.0$, $T_1 = 1150$ K, $T_{0j} = 300$ K, $x = 35.6$ cm $= 89a$, and $\delta_i/a = 3.8$.

Parametric Calculations

Based on the comparisons given above, which cover a wide range of conditions, one can judge the analysis as being "qualified." Either entrainment law seems satisfactory, as long as the higher values are used for the constants. We have used Eq. (9) for parametric calculations, since it is somewhat simpler. It is then possible to make calculations over a range of conditions of interest for scramjet combustors to assess performance and to illustrate the practical utility of the analysis for a situation of current interest.

It is useful to pick a few combinations of conditions and run complete mixing/burning calculations to illustrate flowfield development. The points ($M_\infty = 10$, 15, and 20) on a typical mission profile have been selected, and some predictions are plotted in Fig. 10 assuming $\delta_i/a \ll 1$. One can see that the growth in the average air/fuel ratio along the combustor is nearly the same for all three cases. This is because $(\rho_j u_j/\rho_1 u_1)$ came out nearly the same (0.3–0.4) for all three cases. A long length ($x/a \approx 200$) is required to achieve a reasonable average

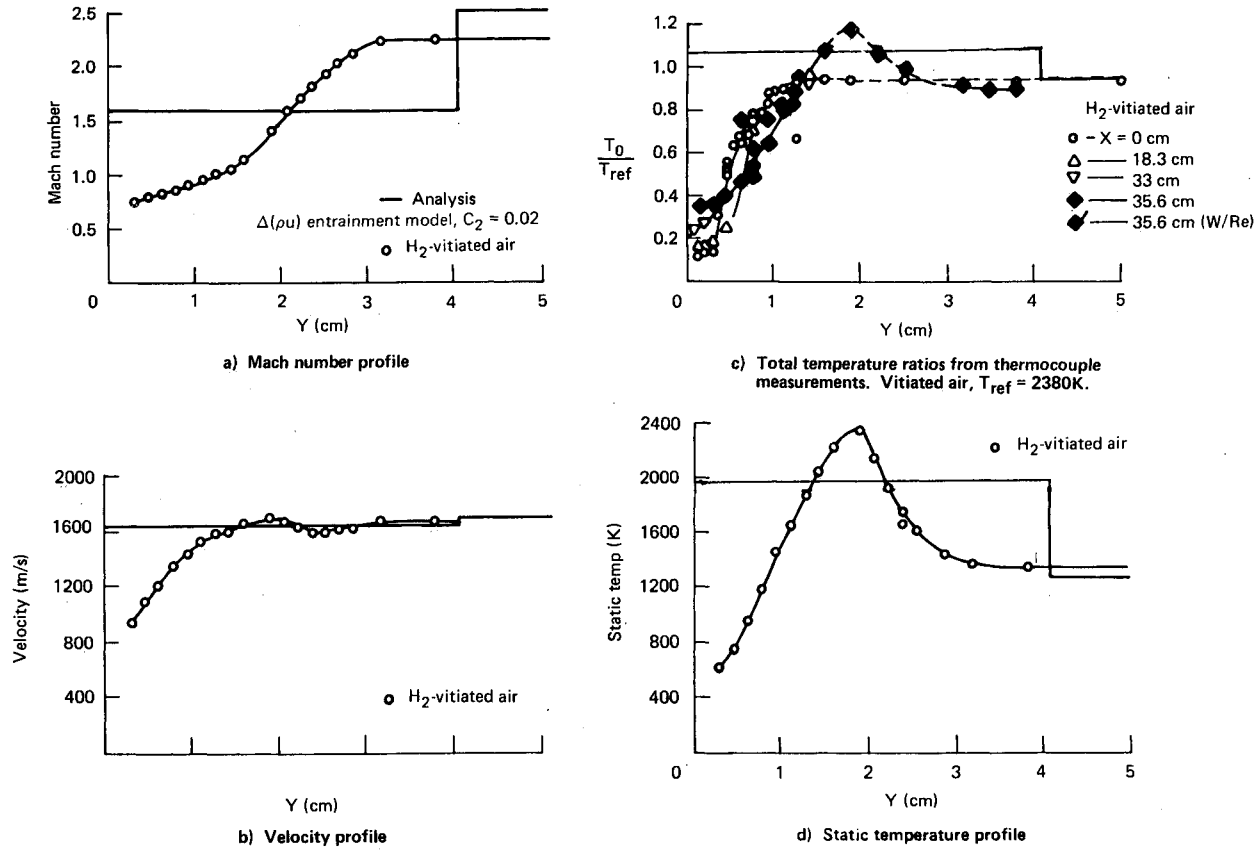

Fig. 7 Comparisons of predictions and data from H_2/air burning experiments of Burrows and Kurkov[9]; $M_1 = 2.5$, $M_j = 1.0$, $T_1 = 1210$ K, $T_{0j} = 300$ K, $x = 35.6$ cm $= 89a$, and $\delta_i/a = 3.8$.

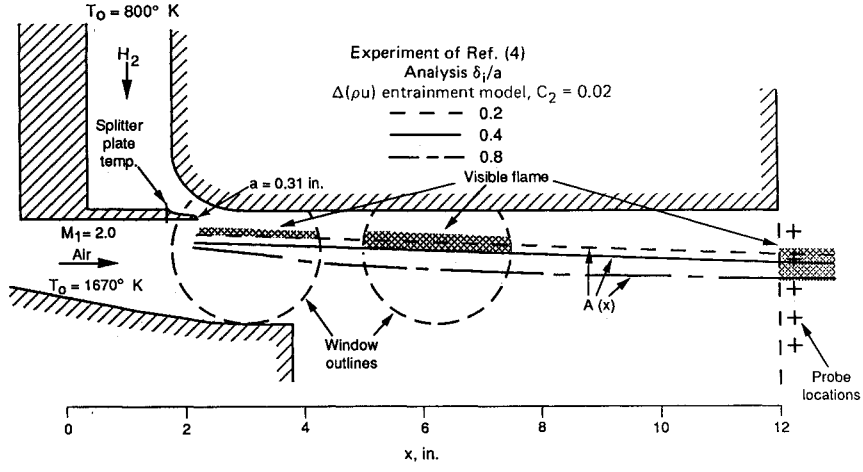

Fig. 8 Experimental apparatus and flame pattern in the tests of Ref. 4 compared to current predictions with assumed values of $\delta_i/a = 0.2$, 0.4, and 0.8; $M_1 = 2$, $M_j = 1.0$.

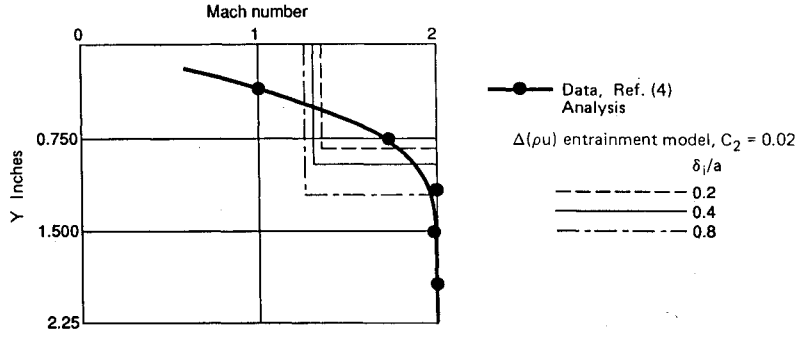

Fig. 9 Mach number distribution at test section exit for $M_1 = 2.0$, $M_j = 1.0$, $T_{01} = 1670$ K, and $T_{0j} = 800$ K for various assumed values of δ_i/a.

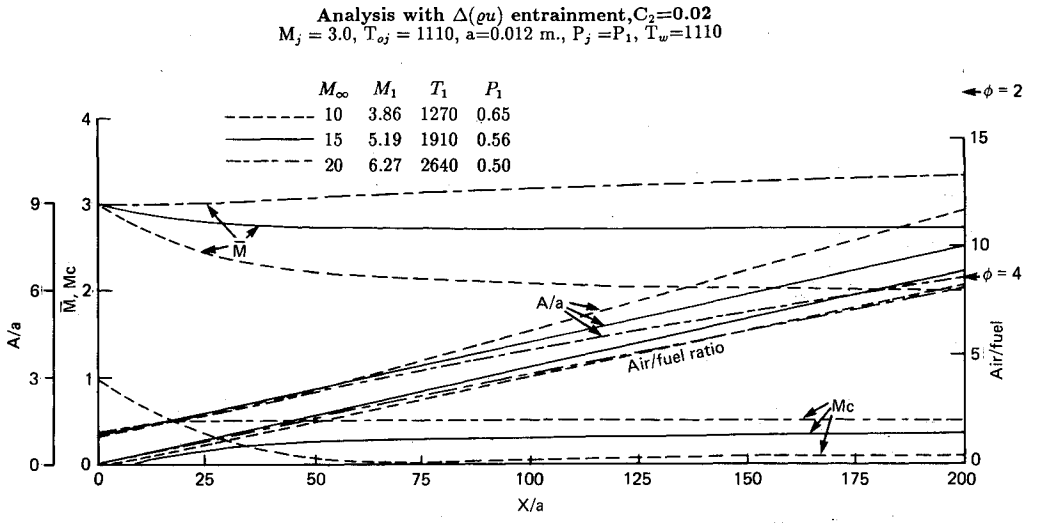

Fig. 10 Predicted variations of some gross variables in the combustor for three flight Mach numbers; $\delta_i/a \ll 1$.

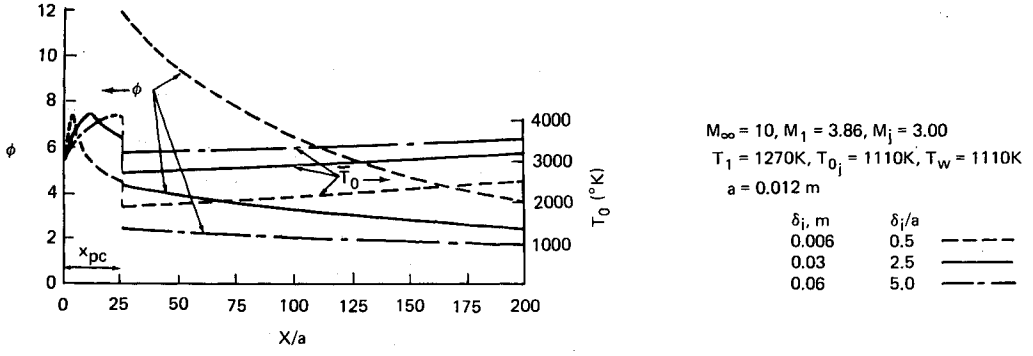

Fig. 11 Predictions of mixture ratio and average total temperature in the viscous region for scramjet combustor at Mach 10 for δ_i/a = 0.5, 2.5, and 5.0.

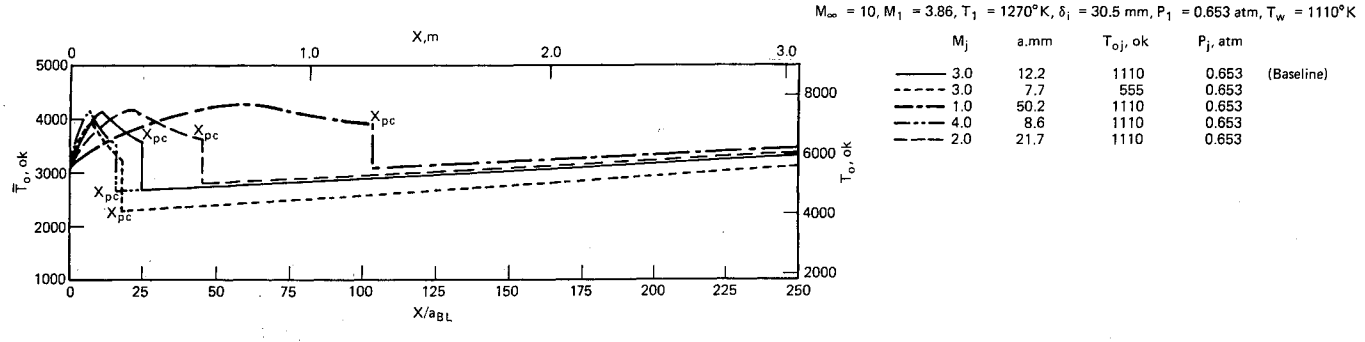

Fig. 12 Effects of injector exit conditions on total temperature variation in the combustor at M_∞ = 10 conditions.

equivalence ratio in the mixing and burning zone. Next, the average Mach number in that zone decreases from M_j for the $M_\infty = 10$ and 15 cases, but it increases for the $M_\infty = 20$ case. This is because $u_1 > u_j$ for the latter case. A convective Mach number effect was included in the calculations, but the conditions were such that it had an effect (very slight) only for the $M_\infty = 20$ case. The figure shows the variation of M_c encountered.

Now, one can consider the effects of an initial boundary layer whose thickness is not small compared to the slot height. For that purpose, we have selected the Mach 10 case with $\delta_i/a = 2.5$ as the baseline condition. We considered δ_i/a of 0.5 to 5 to cover the complete range of probable interest.

The main results can be shown by plots of $T_0(x)$ (the one-dimensional average total temperature in the mixing zone) and $\phi(x)$ in the mixing zone in the Fig. 11. For a "small" initial boundary layer ($\delta_i/a = 0.5$), there is less air in the mixing zone to begin with, and the mixture is rich all the way to $x/a = 200$ and beyond. The temperature is, therefore, also lowest. For a much larger initial boundary layer ($\delta_i/a = 5.0$), there is a lot of hot air in the mixing zone right from the beginning. This results in a leaner, hotter mixture over the whole length studied. Finally, for all these cases, the convective Mach number was never above 0.5.

It is informative to consider some additional parametric variations about the baseline. There are three primary parameters governing the slot injection flow: Mach number M_j; total temperature T_{0j}; and static pressure ratio p_j/p_1. Figures 12 and 13 display some of the influences of M_j and T_{0j} holding p_j and the injected mass flow rate $\dot{m}_j$ constant. Decreasing the slot Mach number to 2.0 or 1.0 requires a larger slot height, which results in a longer potential core length x_{pc}. Increasing M_j has the opposite effect. Decreasing the total temperature of the injectant at a fixed M_j also reduces the slot height and thus x_{pc}. From a practical point of view, one can interpret these results in terms of a length required to reach a certain average

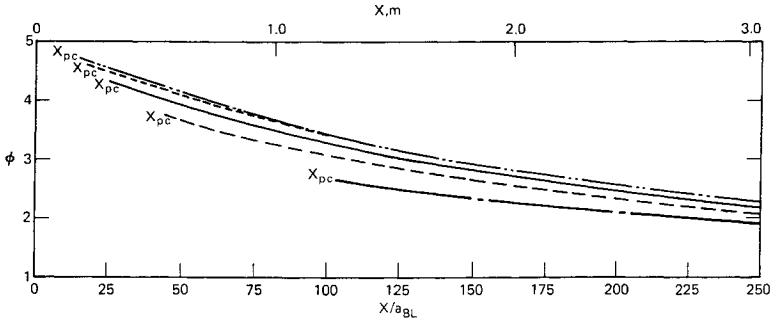

M_∞ = 10, M_1 = 3.86, T_1 = 1270°K, δ_i = 30.5 mm, P_1 = 0.653 atm, T_w = 1110°K

	M_j	a,mm	T_{oj}, ok	P_j, atm	
———	3.0	12.2	1110	0.653	(Baseline)
- - - - -	3.0	7.7	555	0.653	
—·—	1.0	50.2	1110	0.653	
—··—	4.0	8.6	1110	0.653	
— —	2.0	21.7	1110	0.653	
			1110	0.653	

Fig. 13 Effects of injector exit conditions on mixture ratio variation for $M_\infty = 10$ conditions.

mixture ratio in the mixing and burning region. At $M_\infty = 10$, a reasonable target value would be $\phi = 2$. Looking at Fig. 13, it can be seen that the "baseline" case would require a length of about $x/a_{BL} \approx 280$ or $x = 3.4$ m. For example, reducing T_{0j} to 555 K or increasing M_j to 4.0 increases this length to about 3.7 m. Or, decreasing M_j to 2.0 reduces the length to approximately 3.2 m.

Discussion

The results of comparisons of predictions and experiment for nonburning cases, including some with a very large density difference, and H_2/air burning cases demonstrate the adequacy of the new simplified analysis using a $\Delta(\rho u)$ entrainment law with a value of about 0.02 for the mixing rate constant. The same comparisons did not yield an answer to the question of the influence of convective Mach number on wall bounded, mixing flows with a large initial boundary layer, since none of the experiments involved convective Mach numbers high enough (i.e., $M_c \geq 0.5$) to be in the range where such effects have been reported for free shear layers. The results obtained here for cases with sizeable initial boundary-layer thicknesses compared to the slot height are in better agreement with experimental observations than those obtained earlier[22] with an analysis that neglected any direct effect of the initial boundary layer.

The analysis was used to show the influences of initial boundary-layer thickness and injection parameters on combustor flowfield development for a generic scramjet vehicle at a flight Mach number of 10. As might be expected, the influences can be large and important for design purposes.

Calculations that show good agreement with complicated cases such as H_2/air slot mixing and burning experiments can be obtained with this analysis at very modest cost. A complete calculation uses about 1-2 s CPU time on the Amdahl 5890 computer. Thus, this analysis can be useful for design purposes where repeated calculations with parametric variations in the conditions are needed.

Acknowledgment

This work was supported by the Office of Naval Research, Navy Energy and Natural Resources.

References

[1]Visich, M., and Libby, P. A., "Experimental Investigation of Mixing of Mach Number 3.95 Stream in Presence of Wall," NASA TN-D-247, Feb. 1960.

[2]Goldstein, R. J., Eckert, E. R. G., Tsou, F. K., and Haji-Sheikh, A., "Film Cooling with Air and Helium Injection Through a Rearward-Facing Slot into a Supersonic Air Flow," *AIAA Journal*, Vol. 4, No. 6, 1966, pp. 981-985.

[3]Schetz, J. A., and Gilreath, H. E., "Tangential Slot Injection in Supersonic Flow," *AIAA Journal*, Vol. 5, No. 12, 1967, pp. 2149-2154.

[4]Schetz, J. A., and Favin, J., "Ignition and Combustion of Slot Injected Hydrogen in a Supersonic Air Stream," NASA CR-344, 1966.

[5]Petersen, J. B., Jr., McRee, D. I., Adcock, J. B., and Braslow, A. L., "Further Investigation of Effect of Air Injection Through Slots and Porous Surfaces on Flat-Plate Turbulent Skin Friction at Mach 3,"NASA TN-D-3311, N66-20928, March 1966.

[6]Cary, A. M., Jr., and Hefner, J. N., "Film Cooling Effectiveness in Hypersonic Turbulent Flow," *AIAA Journal*, Vol. 8, No. 11, 1970, pp. 2090-2091.

[7]Zakkay, V., Sakell, L., and Parthasarathy, L., "An Experimental Investigation of Supersonic Slot Cooling," *Proceedings of the 1970 Heat Transfer and Fluid Mechanics Institute,* edited by T. Sarpkaya, Stanford Univ. Press, Stanford, CA, pp. 88-103.

[8]Gilreath, H., and Schetz, J. A., "Transition and Mixing in the Shear Layer Produced by Tangential Injection in Supersonic Flow," *Journal of Basic Engineering,* Dec. 1971, pp. 610-618.

[9]Burrows, M. C., and Kurkov, A. P., "Supersonic Combustion of Hydrogen in a Vitiated Air Stream Using Stepped-Wall Injection," AIAA Paper 71-721, June 1971.

[10]Walker, D. A., Campbell, R. L., and Schetz, J. A., "Turbulence Measurements for Slot Injection in Supersonic Flow," AIAA Paper 88-0123, Jan. 1988.

[11]Beckwith, I. E., and Bushnell, D. M., "Calculations by a Finite-Difference Method of Supersonic Turbulent Boundary Layers with Tangential Slot Injection," NASA TN-D-6221, 1971.

[12]Bushnell, D. M., "Calculation of Relaxing Turbulent Boundary Layers Downstream of Tangential Slot Injection," *Journal of Spacecraft and Rockets,* Vol. 8, No. 5, 1971, pp. 550-551.

[13]Miner, E. M., and Lewis, C. H., "Supersonic Turbulent Boundary-Layer Flows with Tangential Slot Injection," AIAA Paper 73-969, 1973.

[14]Murray, A. L., "Supersonic Boundary Layer Flows with Hydrogen Injection and Combustion," M. S. Thesis, Virginia Polytechnic Institute and State Univ., Blacksburg, VA, 1975.

[15]Brown, G. L., and Roshko, A. A., "On Density Effects and Large Structure in Turbulent Mixing Layers," *Journal of Mechanics*, Vol. 64, 1974, Pt. 4, pp. 775-816.

[16]Bogdanoff, D. W., "Compressibility Effects in Turbulent Shear Layers,"*AIAA Journal*, Vol. 21, No. 6, 1983, pp. 926-927.

[17]Padova, C., Boyer, D. W., and Warster, W. H., "Mach Number and Density Effects in the Mixing of Supersonic Jets," JANNAF 14th Plume Technology Meeting, Chemical Propulsion Information Agency, Applied Physics Lab., Laurel, MD, CPIA Pub. 384, Vol. 1, Nov. 1983.

[18]Papamoschou, D., and Roshko, A., "Observations of Supersonic Free Shear Layers," AIAA Paper 86-0162, 1986.

[19]Schetz, J. A., Billig, F. S., and Favin, S., "Simplified Analysis of Supersonic Base Flows Including Injection and Combustion," *AIAA Journal*, Vol. 14, No. 1, 1976, pp. 7-8.

[20]Schetz, J. A., Billig, F. S., and Favin, S., "Approximate Analysis of Axisymmetric Supersonic Base Flows with Injection," *AIAA Journal*, Vol. 18, No. 8, 1980, pp. 867-868.

[21]Schetz, J. A., Billig, F. S., and Favin, S., "Analysis of Base Drag Reduction by Base and/or External Burning," *AIAA Journal,* Vol. 19, No. 9, 1981, pp. 1145-1150.

[22]Schetz, J. A., Billig, F. S., and Favin, S., "Simplified Analysis of Slot Injection in Hypersonic Flow," AIAA Paper 88-3056, July 1988.

[23]Shapiro, A. H., *The Dynamics and Thermodynamics of Compressible Fluid Flow*, Ronald Press, New York, 1953.

[24]Crocco, L., and Lees, L., "A Mixing Theory for the Interaction Between Dissipative Flows and Nearly Isentropic Streams," *Journal of Aeronautical Sciences,* Vol. 19, Oct. 1952, pp. 649-676.

[25]Ferri, A., Libby, P. A., and Zakkay, V., "Theoretical and Experimental Investigation of Supersonic Combustion," *Proceedings of the International Council of the Aeronautical Sciences*, 1962, pp. 1089-1155.